Front. Phys. 12(4), 120502 (2017)
DOI 10.1007/s11467-016-0622-1

RESEARCH ARTICLE

Ratchet motion and current reversal of coupled Brownian motors in pulsating symmetric potentials

Chen-Pu Li[1,2], **Hong-Bin Chen**[3,4], **Zhi-Gang Zheng**[3,4,†]

[1] *Department of Physics, Beijing Normal University, Beijing 100875, China*
[2] *College of Science, Hebei University of Architecture, Zhangjiakou 075000, China*
[3] *Institute of Systems Science (ISS), Huaqiao University, Xiamen 361021, China*
[4] *College of Information Science and Engineering, Huaqiao University, Xiamen 361021, China*
Corresponding Author. E-mail: [†] *zgzheng@hqu.edu.cn.*
Received July 20, 2016; accepted August 29, 2016

In this study, we investigate the collective directed transport of coupled Brownian particles in spatially symmetric periodic potentials under time-periodic pulsating modulations. We find that the coupling between two particles can induce symmetry breaking and consequently collective directed motion. Moreover, the direction of motion can be reversed under certain conditions. The dependence of directed current on various parameters is systematically studied. reverse motion can be achieved by modulating the coupling free length and the phase shift of the pulsating potential. The dynamical mechanism of these transport properties is understood in terms of the effective-potential theory and the space-time transformation invariance. The directed transport of coupled Brownian motors can be manipulated and optimized by adjusting the coupling strength, pulsating frequency, or noise intensity.

Keywords coupled Brownian motors, ratchet, effective potential, symmetric periodic potential, noise

PACS numbers 05.45.Xt, 05.40.-a, 05.60.-k, 02.50.Ey

Frontiers of Physics

1 Introduction

Directed transport of non-equilibrium Brownian particles is an important topic in many different scenarios [1–4]. Directed transport requires the breaking of detailed balance as well as the breaking of symmetry. Symmetry breaking includes the breaking of spatial symmetry of the periodic potential field and the breaking of temporal symmetry of driving, and the mechanism of symmetry-breaking-induced ratchet motion has been extensively studied in recent years [5–8]. In fact, it has been revealed that the coupling of particles can also lead to symmetry breaking and rich ratchet effects [9, 10]. Therefore, it is necessary to consider the influence of the coupling of particles in systems composed of a number of interacting particles. Examples of such coupled physical systems include the diffusion of dimers on surfaces [11–13], sliding friction [14, 15], biological molecular motors [16–21], and diffusion of colloidal particles [22]. The existence of interactions introduces complexity in the dynamics of the Brownian particles. Bao *et al.* investigated the dynamical mechanism of the ratchet motion of elastically coupled two-head Brownian motors in flashing asymmetric potential fields, and they found that the coupling can assist directed motion. Furthermore, they theoretically interpreted their results in terms of the motion of the mass center in an effective potential [23]. Zheng *et al.* systematically explored the collective-directed transport of interacting Brownian motors in one- and two-dimensional periodic potentials. They revealed that the coupling of particles can induce various types of symmetry breaking, e.g., the coupling symmetry breaking and spatiotemporal symmetry breaking, which lead to collective directed transport behaviors [9, 24]. Moreover, they revealed that the coupling can transform the energy in one dimension to another direction and induce collective directed transport [25]. Reimann and colleagues studied the ratchet motion of harmonically coupled motors in a flashing symmetric potential under the action of Gaussian white noise and analyzed the possibility of the ratchet effect through the manipulation of internal degrees of freedom in terms of the effect potential method [26].

Molecular motors are a big family of proteins that play important roles for realizing cellular transport processes. A large sub-family among these different pro-

tein motors possesses the dimer structure in which each motor protein is composed of two interacting identical monomers and every monomer experiences the cyclic ATP hydrolyzing process [27, 28]. A deep understanding of the collective ratcheting motion, stepping distribution, and current reversal of two-head molecular motors has been a topic of focus in recent decades. Early studies on the motion of molecular motors were mainly based on the single-particle picture, in which the motion of molecular motors is simplified to the motion of a Brownian particle in a ratchet potential. Much less effort has been directed towards the role of prototype structure of molecular motors, especially the symmetry breaking of two heads induced by various factors. It was experimentally found that the coupling between two motor protein heads, which do not act independently but alternate in a sequential manner such that their catalytic cycles are out of phase [29, 30], plays a significant role in achieving directed motion and even reversed motion. We noticed an important fact related to the symmetry breaking of dimer molecular motors: the hydrolysis processes of two heads are continuous while asynchronous, which may lead to the dynamical asymmetry of the two motors. This gives us a hint for setting up the ratchet model of coupled motors in a symmetric potential field under temporally periodic pulsations.

In this study, we investigate the directed transport of two elastically interacting Brownian motors in a spatially symmetric and temporally modulated pulsating periodic potential. We are interested in the emergence of current reversal and its mechanism. A key point in inducing the directed motion of coupled motors in symmetric potentials is the asynchrony property of the pulsations on two motors though they are pulsated in the same manner. Theoretically, the transport behaviors, such as the mechanism of ratcheting effect and current reversal, can be analyzed in terms of the effective-potential theory and the space-time invariance of the system. We find that the shifting direction of the effective potential wells in one pulsating period determines the collective directed motion as well as the current reversal. Moreover, various parameters such as the coupling strength, free length, pulsation frequency, pulsation phase mismatch, and the noise intensity may substantially influence the ratchet motion of coupled Brownian motors, which allows the easy optimization and manipulation of collective directed transport through the modulations of these parameters.

2 The coupled pulsating-potential Brownian Motor Model

Let us consider the Brownian motion of two elastically interacting motors in a symmetric periodic potential field. For simplicity, we consider the overdamped Brownian motion under Gaussian white noise. In contrast to the usually adopted steady periodic potential field, we consider here the temporally modulated potential by pulsating the potential height. The equations of motion of two mutually coupled motors can be written as

$$\dot{x_i} = -\frac{\partial V(x_i)}{\partial x_i} f_i(t) - \frac{\partial U_0}{\partial x_i} + \xi_i(t), \quad i = 1, 2, \tag{1}$$

where x_i is the coordinate of the i-th motor and $V(x)$ is the periodic potential originating from the interaction between the motor protein and the track.

$$V(x) = \frac{V_0}{2}\left[1 - \cos\left(\frac{2\pi}{L}x\right)\right], \tag{2}$$

where L is the spatial period of the potential field. Note that the potential given by (2) is spatially symmetric. $U_0(x_1, x_2)$ denotes the interaction potential of two motor heads and is set to the following harmonic potential for simplicity:

$$U_0(x_1, x_2) = \frac{1}{2}k(x_1 - x_2 - a)^2, \tag{3}$$

where k is the coupling strength and a is the free length. We consider the external drives on two heads with the simplest uncorrelated Gaussian white noise, $\xi_1(t)$ and $\xi_2(t)$, as follows:

$$\begin{aligned} &\langle \xi_i(t) \rangle = 0, \\ &\langle \xi_i(t)\xi_j(t') \rangle = G\delta_{ij}\delta(t - t'), \quad i, j = 1, 2, \end{aligned} \tag{4}$$

where $G = 2k_BT$ represents the noise intensity. The function $f_i(t)$ is the periodic modulation of the potential field. This is biologically related to the modulation of the height of the potential field, which results from the interaction between ATP and the two heads. The two heads usually stay at different ATP-hydrolysis states at the same time, resulting in different coupling between heads and the substrate potentials. Without losing generality, we assume there exists a phase difference θ between two modulation functions $f_{1,2}(t)$, i.e.,

$$f_1(t) = 1 + \cos(\omega t + \theta), \tag{5}$$

$$f_2(t) = 1 + \cos(\omega t), \tag{6}$$

Here, ω is the pulsating frequency of the potential. Hence, we set up a Brownian-motor model that describes the motion of two coupled heads in a pulsating symmetric potential. It should be noted that there exists no symmetry breaking mechanism for each head, and no directed motion can occur in the absence of mutual coupling between two heads. The emergence of ratchet motion should be accomplished through the coordination of two motors. It is significant to study the possibility

of ratchet motion through the cooperation of two heads. One is also interested in the dependence of the transport on various parameters. Current reversal is an important issue in studies of Brownian motors, and it is necessary to explore such behaviors in two-head motors. In the following discussions, we investigate these questions through both theoretical computations and numerical simulations.

3 Effective potential theory for strongly-coupled motors

A natural idea when dealing with the cooperative ratcheting effect of two coupled Brownian motors is to decrease the degrees of freedom of the system to obtain a low-dimensional description, especially in the single-particle scenario. If this is possible, the dynamics of the coupled system can be modeled in terms of the motion of one particle in an effective potential field. This approach is valid as long as the coupling strength is sufficiently large, i.e., $k \gg \omega$. By introducing the mass-center coordinate $X = (x_1 + x_2)/2$ and the lattice coordinate $Y = x_1 - x_2$, one can find that the motion can be well described by the equation of motion of X by introducing the effective potential $V_{eff}(X,t)$. Let us accomplish this step by step. By introducing (X,Y), one can transform Eq. (1) to

$$\dot{X} = \frac{1}{2}\left[-\frac{1}{2}\frac{\partial V(X+\frac{Y}{2})}{\partial X} - \frac{\partial V(X+\frac{Y}{2})}{\partial Y}\right] f_1(t) + \frac{1}{2}\left[-\frac{1}{2}\frac{\partial V(X-\frac{Y}{2})}{\partial X} + \frac{\partial V(X-\frac{Y}{2})}{\partial Y}\right] f_2(t) + \xi_X(t), \tag{7}$$

$$\dot{Y} = \left[-\frac{1}{2}\frac{\partial V(X+\frac{Y}{2})}{\partial X} - \frac{\partial V(X+\frac{Y}{2})}{\partial Y}\right] f_1(t) + \left[\frac{1}{2}\frac{\partial V(X-\frac{Y}{2})}{\partial X} - \frac{\partial V(X-\frac{Y}{2})}{\partial Y}\right] f_2(t) - 2k(Y-a) + \xi_Y(t), \tag{8}$$

where

$$\langle \xi_X(t)\xi_X(t')\rangle = (G/2)\delta(t-t'),$$
$$\langle \xi_Y(t)\xi_Y(t')\rangle = 2G\delta(t-t').$$

It can be easily seen that, when the coupling strength k is sufficiently large, the term $2k(Y-a)$ implies a much faster decay of the coordinate Y as compared with X. Therefore, Y is a fast variable and can be adiabatically eliminated in terms of the slaving principle proposed by H. Haken. This means that one can set $\mathrm{d}Y/\mathrm{d}t \approx 0$, and the motion of two particles can be studied based on

$$\dot{X} = -V'_{eff}(X,t) + \xi_X(t), \tag{9}$$

where the effective potential field can be written as [10, 23, 26]

$$V_{eff}(X,t) = -\frac{1}{2}k_BT \ln\left(\int_{-\infty}^{\infty} \rho(X,Y,t)\mathrm{d}Y\right). \tag{10}$$

Here,

$$\rho(X,Y,t) = \exp\left(-\frac{U(X,Y,t)}{k_BT}\right) \tag{11}$$

$$U(X,Y,t) = \frac{1}{2}k(Y-a)^2 + V\left(X+\frac{Y}{2}\right) f_1(t) + V\left(X-\frac{Y}{2}\right) f_2(t). \tag{12}$$

Therefore, we can simplify the complicated dynamics of coupled systems to the motion of one degree of freedom by introducing an effective potential. This can be the starting point of theoretical discussions of coupled Brownian motors. An effective potential $V_{eff}(X,t)$ is shown in Fig. 1 for parameters $\omega = 1$, $k = 50$, $\theta = \pi/5$, $a = 0.4$, $G = 0.1$, $V_0 = 1$, and $L = 1$. It will be shown in the following discussions that the properties of the effective potential can be adapted to the analysis of the mechanism of collective directed transport.

The numerical simulation of Eq. (1) may not only lead to the dynamics and consequently various quantities such as average displacement and average velocity, but also test the validity of the effective-potential approach. Moreover, we can obtain results through numerical simulation for cases in which the effective potential method does not apply. In the present work the second-order Runge–Kutta algorithm is adopted [31, 32], and the number of ensembles $N = 1000$ with the time step $dt = 0.001$. Throughout the numerical simulations, we set $V_0 = 1$ and $L = 1$. The average velocity or the current can be obtained by executing both ensemble and time averages on the instantaneous velocity:

$$v = \langle \dot{x} \rangle = \lim_{t\to\infty} \frac{1}{NT} \sum_{i=1}^{N} \int_0^t \dot{x}_i(t')\mathrm{d}t'. \tag{13}$$

4 Collective directed transport and current reversal

4.1 Unidirectional stepping motion of Brownian motors

For a single motor, no directed motion exists under the action of the symmetric potential $V(x)$ and the Gaussian white noise $\xi(t)$. The coupling between two motors may lead to symmetry breaking in the effective potential and, furthermore, directed motion. The peak of the effective potential given by Fig. 1 first increases and then

decreases in a period. Moreover, the bottom of the potential experiences a shift to the right (see the black arrow in Fig. 1). This provides a larger probability of diffusion to the right of the coupled motors and makes the directed motion possible. Figure 2 shows the evolution of the position of the mass center. It can be seen that the coupled motors experience a stepping forward motion with an equal step to the period L of the potential $V(x)$. The motors stay randomly for a while before the next stepping motion. This stepping behavior is a cooperation among various different factors, and the driving of stochastic noise leads to the randomness of the residence time and stepping.

4.2 Current reversal induced by coupling

The presence of coupling between two motor heads not only results in the cooperative directed motion, but also plays a significant role in influencing the current. The direction of the current can even be determined by the free length of the coupling potential. Fig. 3(a) shows the variation of the average current with the coupling free length a for other parameters given in the plot, where four curves correspond to the coupling strengths $k = 5$, 10, 50, and 1000, respectively. These four curves have the same feature that the current $v > 0$ when $0 < a < 0.5$ while $v < 0$ for $0.5 < a < 1$. These curves are antisymmetric about $a = 0.5$. This indicates that, with the variation of the free length a, the directed motion can be reversed. For a given coupling strength, there exists an optimal free length a_{max} for the system possessing the largest current. For larger coupling strength k, the optimal a_{max} is larger.

The interesting current-reversal behavior described above can be theoretically interpreted in terms of the effective potential approach for the strong-coupling case. Figures 3(b), (c), and (d) show the curves of the effective potential $V_{eff}(X)$ at different moments for the free lengths $a = 0.4$, 0.5, and 0.6, respectively, where the other parameters are $\omega = 1$, $k = 50$, $\theta = \pi/5$, $G = 0.1$.

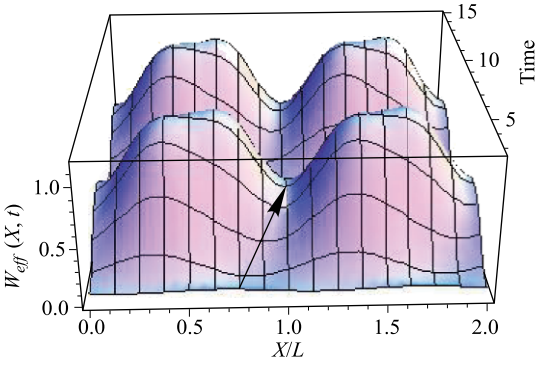

Fig. 1 The effective potential $V_{eff}(X,t)$.

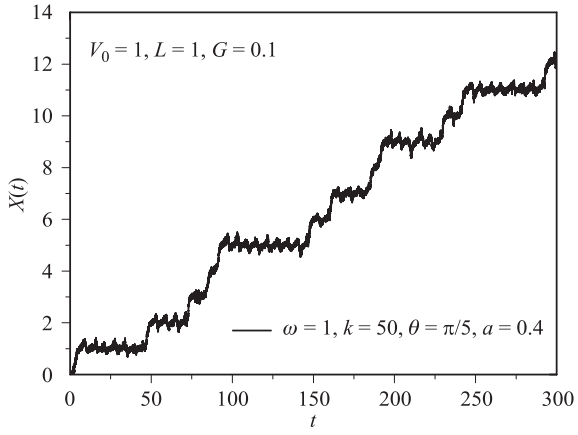

Fig. 2 The stepping motion of the mass center of the coupled Brownian motors.

It can be found that, when $0 < a < 0.5$ (see Fig. 3(b)), the height of the effective potential first increases and then decreases with time in one pulsating period; meanwhile, the position of the potential valley shifts to the right (see the shift from A to B and C in Fig. 3(b)), which gives a larger diffusion probability to the right direction. This symmetry breaking leads to a net current to the right. When $a = 0.5$, the potential height follows a similar change, but the bottom has a symmetric shift to both directions, as shown by the two green curves A-B1-C1 and A-B2-C2 in Fig. 3(c). In this case, the probabilities to the right equal those to the left, indicating null-directed motion. Figure 3(d) shows the curves of the effective potentials for $0.5 < a < 1$. It can be observed that the evolutional behaviors of the effective potential exhibit a reversed tendency as compared the case of $0 < a < 0.5$, and the potential bottom moves as A-B-C to the left. This naturally leads to a current reversal of the coupled motors when $0 < a < 0.5$. Therefore, the mechanism of collective directed motion and the current reversal can be well understood via the effective potential theory.

The effective potential approach provides a way for evaluating the mechanism of directed motion of coupled Brownian motors for strong-coupling scenarios, where the transport depends crucially on the tendency of shift of the potential bottom. This naturally gives us a hint for introducing an *effective asymmetry coefficient* Δ_{eff}, which can be defined as

$$\Delta_{eff} = X_{2min} - X_{1min}, \tag{14}$$

where X_{1min} is the position of the minimum of the first-half period average of the effective potential $V_{eff}(X,t)$, i.e.,

$$V_{eff}(X) = \frac{1}{T_0/2}\int_0^{\frac{T_0}{2}} V_{eff}(X,t)\mathrm{d}t,$$

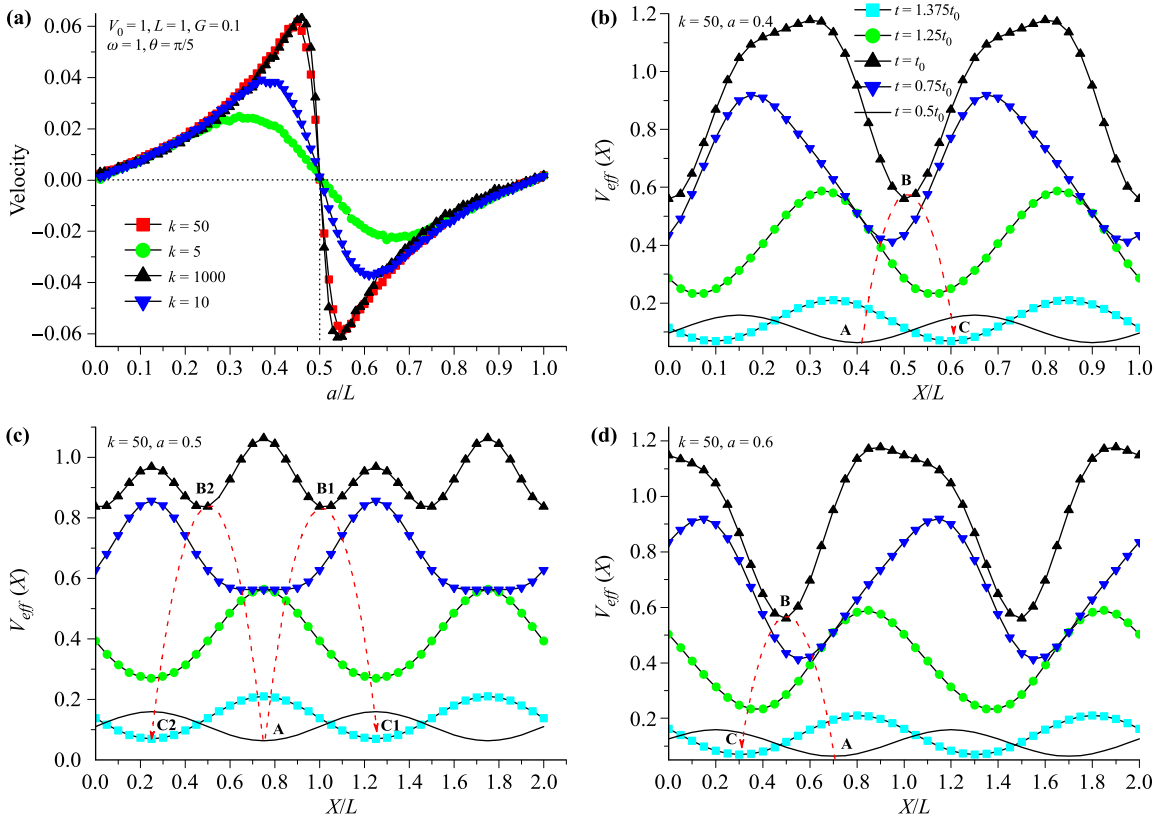

Fig. 3 **(a)** The average velocity varying with the free length a; All curves are anti-symmetric about $a = L/2$. **(b)** The shifting motion of the effective potential well in one pulsating period for $a = 0.4L$, and a shift from A to B then to C can be observed. **(c)** The shifting motion of the effective potential well in one pulsating period for $a = 0.5L$, and a symmetric shift A-B1-C1 and A-B2-C2 can be observed. **(d)** The shifting motion of the effective potential well in one pulsating period for $a = 0.6L$, and a shift from A to B then to C can be observed.

and X_{2min} is the position of the minimum of the second-half period average of the effective potential $V_{eff}(X,t)$, i.e.,

$$V_{eff}(X) = \frac{1}{T_0/2}\int_{\frac{T_0}{2}}^{T_0} V_{eff}(X,t)\mathrm{d}t.$$

When $\Delta_{eff} > 0$, the minimum of the effective potential $V_{eff}(X,t)$ moves to the right in one pulsating period. In this case, the diffusion of two coupled Brownian motors has a larger probability to the right than that to the left when the barrier of the effective potential is not sufficiently high, resulting in a positive average velocity. In contrast, when $\Delta_{eff} < 0$, a similar argument can predict a negative average velocity of coupled Brownian motors. The situation $\Delta_{eff} = 0$ indicates that the shifts of the valley of $V_{eff}(X,t)$ in both directions are symmetric, corresponding to a null velocity of coupled motors. Fig. 4 plots the variation of the effective asymmetry coefficient Δ_{eff} with the free length a for different coupling strengths, which agrees well with the above analysis. It can also be found from Fig. 4 that, for both regimes $0 < a < L/2$ and $L/2 < a < L$, the absolute value of the asymmetry coefficient $|\Delta_{eff}|$ increases with the increase of the coupling strength k, which qualitatively implies that the average velocity of the ratchet motion of coupled motors increases when the coupling strength is increased. For sufficiently strong coupling strengths, e.g., $k = 500$ and 1000, as shown in Fig. 4, Δ_{eff} saturates to the largest value. This result is in agreement with the dependence of the average velocity on the free length for the strong-coupling case shown in Fig. 3(a).

The current reversal shown above can also be well understood through the analysis of the space-time transformation invariance of the dynamical Eq. (1) [24, 26, 33, 34]. By rewriting Eq. (1) with a superscript corresponding to the value of coupling free length a as

$$\begin{aligned}\dot{x}_1^{(a)} &= -V'(x_1)f_1(t) - k(x_1 - x_2 - a) + \xi_1(t),\\ \dot{x}_2^{(a)} &= -V'(x_2)f_2(t) + k(x_1 - x_2 - a) + \xi_2(t).\end{aligned} \quad (15)$$

By replacing the free length a by $nL - a$, where $n \in \mathbb{Z}$, one obtains

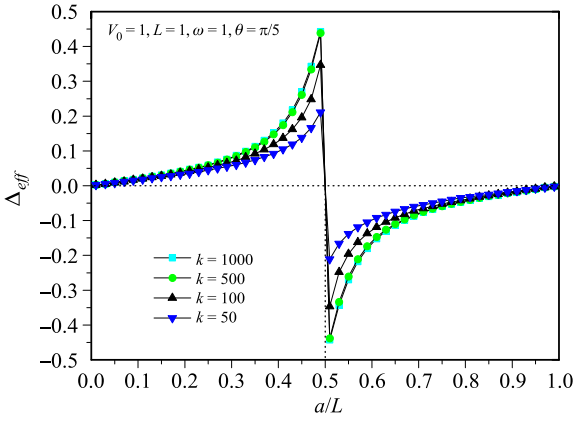

Fig. 4 The effective asymmetry coefficient against the coupling free length for different coupling strengths.

$$\begin{aligned}\dot{x}_1^{(nL-a)} &= -V'(x_1)f_1(t) - k((x_1 - nL) - x_2 + a) + \xi_1(t),\\ \dot{x}_2^{(nL-a)} &= -V'(x_2)f_2(t) + k((x_1 - nL) - x_2 + a) + \xi_2(t).\end{aligned} \tag{16}$$

By introducing $x_{11} = x_1 - nL$ into Eq. (16) and considering the periodicity of the potential $V(x)$, we have

$$\begin{aligned}\dot{x}_{11}^{(nL-a)} &= -V'(x_{11})f_1(t) + k(x_2 - x_{11} - a) + \xi_1(t),\\ \dot{x}_2^{(nL-a)} &= -V'(x_2)f_2(t) - k(x_2 - x_{11} - a) + \xi_2(t).\end{aligned} \tag{17}$$

By using the transformation $x_{11} \to x_1$ and $t \to -t$, we obtain from Eq. (17)

$$\begin{aligned}-\dot{x}_1^{(nL-a)} &= -V'(x_1)f_1(-t) + k(x_2 - x_1 - a) + \xi_1(-t)\\ &= -V'(x_1)\left[1 + \cos\left(\omega\left(t - \frac{\theta}{\omega}\right)\right)\right]\\ &\quad + k(x_2 - x_1 - a) + \xi_1(t),\\ -\dot{x}_2^{(nL-a)} &= -V'(x_2)f_2(-t) - k(x_2 - x_1 - a) + \xi_2(-t)\\ &= -V'(x_2)[1 + \cos(\omega t)] - k(x_2 - x_1 - a) + \xi_2(t).\end{aligned} \tag{18}$$

One further inserts $t' = t - (\theta/\omega)$ into Eq. (18) and obtains

$$\begin{aligned}-\dot{x}_1^{(nL-a)} &= -V'(x_1)[1 + \cos(\omega t')]\\ &\quad + k(x_2 - x_1 - a) + \xi_1(t')\\ &= -V'(x_1)f_2(t') + k(x_2 - x_1 - a) + \xi_1(t'),\\ -\dot{x}_2^{(nL-a)} &= -V'(x_2)[1 + \cos(\omega(t' + \frac{\theta}{\omega}))]\\ &\quad - k(x_2 - x_1 - a) + \xi_2(t')\\ &= -V'(x_2)[1 + \cos(\omega t' + \theta)]\\ &\quad - k(x_2 - x_1 - a) + \xi_2(t')\\ &= -V'(x_2)f_1(t') - k(x_2 - x_1 - a) + \xi_2(t').\end{aligned} \tag{19}$$

By exchanging indices as $x_1 \leftrightarrow x_2$ and comparing with Eq. (15), one obtains

$$\begin{aligned}-\dot{x}_2^{(nL-a)} &= -V'(x_2)f_2(t') + k(x_1 - x_2 - a) + \xi_2(t')\\ &= \dot{x}_2^{(a)},\\ -\dot{x}_1^{(nL-a)} &= -V'(x_1)f_1(t') - k(x_1 - x_2 - a) + \xi_1(t')\\ &= \dot{x}_1^{(a)}.\end{aligned} \tag{20}$$

Thus, one has

$$\begin{aligned}-v^{(nL-a)} &= -\frac{1}{2}(\dot{x}_1^{(nL-a)} + \dot{x}_2^{(nL-a)})\\ &= v^{(a)} = \frac{1}{2}(\dot{x}_1^{(a)} + \dot{x}_2^{(a)}).\end{aligned} \tag{21}$$

This is interpreted as the anti-symmetry property of the average velocity against the coupling free length a, shown in Fig. 3(a). When $a = nL/2$, one obviously has $-v^{(nL/2)} = v^{(nL/2)}$, which naturally implies $v^{(nL/2)} = 0$. The above analysis of the space-time transformation invariance agrees well with that in terms of the effective-potential theory.

4.3 Current reversal induced by pulsation phase shift

In the above discussions, we observed the reversal of directed motion by modulating the coupling free length. In fact, directed motion can also be reversed by modulating the phase difference θ between the pulsation of the potential of two motors. This reversal is still achieved through the collaboration of two motor heads. In Fig. 5(a), the current is computed against the phase shift θ for $\omega = 0.5$, 1, and 3, and other parameters are $G = 0.1$, $k = 50$, and $a = 0.4$. Several interesting phenomena can be clearly found. First, the v–θ curves are anti-symmetric about $\theta = \pi$, and $v > 0$ when $0 < \theta < \pi$ and $v < 0$ when $\pi < \theta < 2\pi$. Second, there exists an optimal phase shift θ_{max} for which the coupled motors possess the greatest velocity. It can be found that, for different pulsating frequencies ω, the optimized phase shift θ_{max} is different.

The mechanism of current reversal induced by pulsation phase shift can also be well understood with the help of effective potential theory. Let us study the effective-potential curves at different times for different phase shifts θ, which are shown in Fig. 5(b), (c), and (d) for $\theta = \pi/5$, $\theta = \pi$, and $\theta = 9\pi/5$, respectively. The other parameters are $\omega = 1$, $k = 50$, $a = 0.4$, and $G = 0.1$. As shown in Fig. 5(b), when $0 < \theta < \pi$ (e.g.,$\theta = \pi/5$), the current of the coupled motors is positive, and one can find that the position of the minimum of the effective potential experiences a shift from A to the right (see C) within a pulsating period. When $\theta = \pi$, as shown in Fig. 5(c), there is a symmetric shift of the potential bottom from A to B and C and then back to A in one pulsating period, i.e., no net shift occurs during the pulsations of the potential. Thus, the diffusion probability

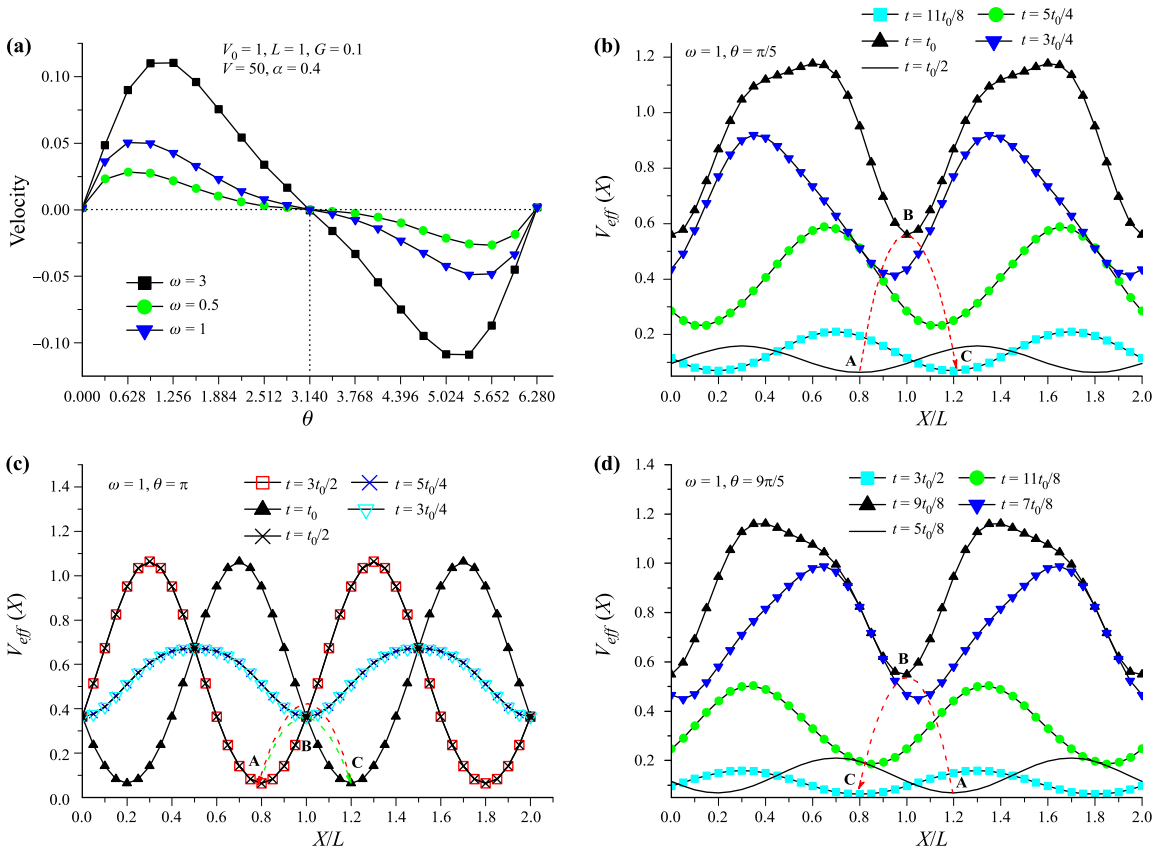

Fig. 5 **(a)** The average velocity varying with the phase difference between pulsations of two particles; All curves are anti-symmetric about $\theta = \pi/2$. **(b)** The shifting motion of the effective potential well in one pulsating period for $\theta = \pi/5$, and a right shift from A to B then to C is observed. **(c)** The shifting motion of the effective potential well in one pulsating period for $\theta = \pi$, and a symmetric shift A-B-C-B-A is observed. **(d)** The shifting motion of the effective potential well in one pulsating period for $\theta = 9\pi/5$, and a left shift from A to B then to C is observed.

of coupled motors to the left equals that to the right, resulting in a null net transport current. As $\pi < \theta < 2\pi$ (for example, $\theta = 9\pi/5$ in Fig. 5(d)), there is a negative shift from A to C in one pulsation period, and the current is reversed.

The current reversal induced by the phase shift can also be well analyzed in terms of the above space-time transformation invariance of dynamical equations (1). Let us rewrite Eq. (1) with a superscript corresponding to the value of phase difference θ as

$$\begin{aligned}\dot{x}_1^{(\theta)} &= -V'(x_1)f_1(t) - k(x_1 - x_2 - a) + \xi_1(t)\\ &= -V'(x_1)[1+\cos(\omega t+\theta)] - k(x_1-x_2-a)+\xi_1(t),\\ \dot{x}_2^{(\theta)} &= -V'(x_2)f_2(t) + k(x_1 - x_2 - a) + \xi_2(t)\\ &= -V'(x_2)[1 + \cos(\omega t)] + k(x_1 - x_2 - a) + \xi_2(t).\end{aligned} \tag{22}$$

By replacing the phase shift θ by $2n\pi - \theta$ ($n \in \mathbb{Z}$) and considering the periodicity of the pulsation function $f_i(t)$, one obtains

$$\begin{aligned}\dot{x}_1^{(2n\pi-\theta)} &= -V'(x_1)[1 + \cos(\omega t - \theta)]\\ &\quad -k(x_1 - x_2 - a) + \xi_1(t),\\ \dot{x}_2^{(2n\pi-\theta)} &= -V'(x_2)[1 + \cos(\omega t)]\\ &\quad +k(x_1 - x_2 - a) + \xi_2(t).\end{aligned} \tag{23}$$

We further execute a time reversal $t \to -t$ and obtain

$$\begin{aligned}-\dot{x}_1^{(2n\pi-\theta)} &= -V'(x_1)[1 + \cos(\omega t + \theta)]\\ &\quad -k(x_1 - x_2 - a) + \xi_1(t)\\ &= -V'(x_1)f_1(t) - k(x_1 - x_2 - a) + \xi_1(t)\\ &= \dot{x}_1^{(\theta)},\\ -\dot{x}_2^{(2n\pi-\theta)} &= -V'(x_2)[1 + \cos(\omega t)]\\ &\quad +k(x_1 - x_2 - a) + \xi_2(t)\\ &= -V'(x_2)f_2(t) + k(x_1 - x_2 - a) + \xi_2(t)\\ &= \dot{x}_2^{(\theta)}.\end{aligned} \tag{24}$$

Therefore, one can easily find that

$$v^{(\theta)} = -v^{(2n\pi-\theta)}.$$

This implies that the relation between the velocity of the coupled Brownian motors and the modulation mismatch θ obeys an anti-symmetric property. For the special choice $\theta = n\pi$, one has $v^{(n\pi)} = -v^{(n\pi)}$, which leads to an unbiased motion of the coupled motors, i.e., $v^{(n\pi)} = 0$. These results agree well with the effective-potential analysis.

5 Optimization and manipulation of collective directed transport

It is interesting to investigate the dependence of the motor motion on the coupling strength between two motor heads. Figure 6(a) plots the variation of the average velocity of the coupled motors with the coupling strength for $\omega = 1.0$, $\theta = \pi/5$, and $a = 0.4$. One can find that, when the coupling strength k is small, the motion can be considered as a simple composition of two single motors, where each particle is immersed in the common symmetric periodic potential and Gaussian white noise. In this case, the average velocity of each particle is zero, as deduced from Curie's principle, which leads to the null directed motion of the coupled system. This analysis is consistent with the result shown in Fig. 6(a) for the behavior of the velocity in the weak-coupling regime, i.e., $k < 1$. For the case of strong coupling, two motor heads have a synchronized cooperation, which may lead to higher-efficiency directed transport. Figure 6(b) shows the collaboration mechanism by relying on the effective potential of the system, where the snapshots of the effective potential for $k = 2 \times 10^3$ are given at different moments in one pulsating cycle. It can be seen that, in the strong-coupling case, the height of the effective potential increases first and then decreases, and the position of the potential valley experiences a shift from A to C. This net shift results in a directed motion of the coupled motor. It can also be seen from Fig. 6(a) that the average velocity saturates as the coupling strength is further increased. In biological molecular motors, the coupling between two motor heads originates from the binding of the dimer structure of the motor protein and can be manipulated using chemical or physical methods. Therefore, the directed transport can be facilitated by adjusting the coupling strength, which is possible in practical situations.

The manipulation of external drives, such as the pulsation $f_i(t)$, can be a better choice for optimizing directed transport. The pulsating frequency ω can be a control parameter in practice. Figure 7 plots the dependence of the average velocity on the pulsating frequency ω, where $G = 0.1$, $k = 50$, $a = 0.4$, and $\theta = \pi/5$. One may find that the average velocity is small for a small ω (e.g., $\omega = 0.1$). This is because the modulation of the substrate potential $f_i(t)$ is so slow that the particles cannot 'feel'

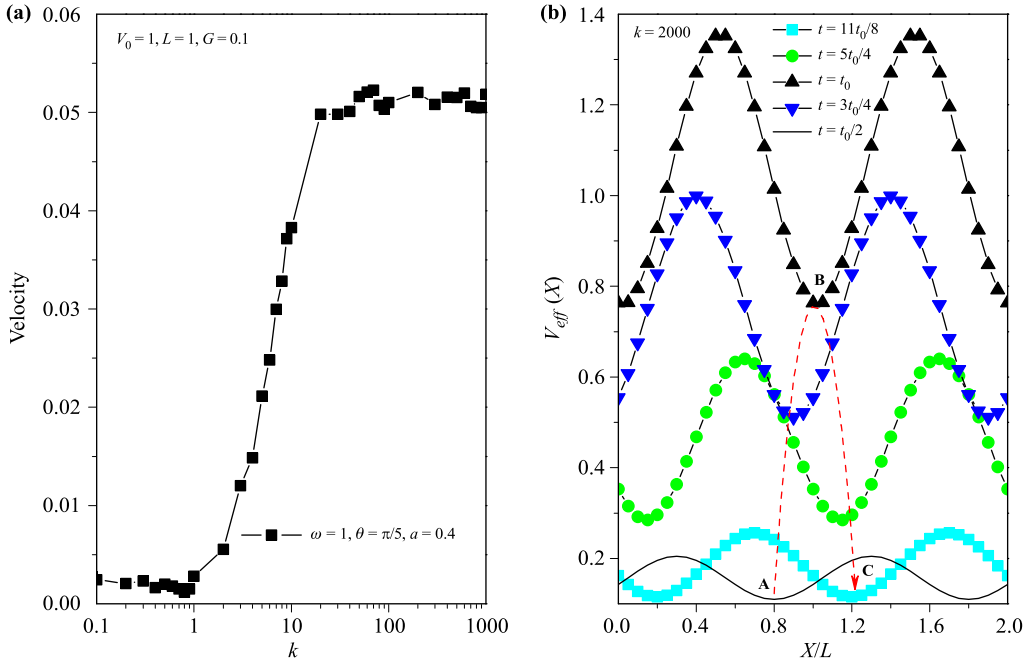

Fig. 6 **(a)** The average velocity of coupled motors against the coupling strength for $\omega = 1.0$, $\theta = \pi/5$, $a = 0.4$ and $G = 0.1$. **(b)** The snapshots of the effective potential at different moment of one pulsating period for the coupling strength $k = 2 \times 10^3$. Other parameters are the same as (a). A right-hand shift A-B-C of the potential valley can be observed.

the change within the time scale of its relaxation, and particles cannot surpass the potential mountain with the help of the modulation. For high-frequency modulations, e.g., when $\omega = 100$, the modulation of the potential $f_i(t)$ is too fast and the particles do not have sufficient time to respond to the pulsation, resulting in the absence of directed motion. An optimal pulsating frequency ω_{max} is, thus, expected for the system possessing the maximized directed velocity, as shown in Fig. 7.

Noise plays a significant role in the nonequilibrium transport of particles. In molecular motors, the existence of noise implies the coupling between motors and the environment via biochemical reactions. Figure 8 plots the average velocity of coupled Brownian motors against the noise strength G for $k = 50.0$, $\theta = \pi/5$, and $a = 0.4$. The curve indicates a strong optimized dependence of the motor motion on the noise intensity. For very weak noises, the Brownian motors cannot obtain sufficient energy to surpass the potential barrier. On the other hand, if the noise intensity is so large that the contributions of noises to the motion in both directions are unbiased, one still cannot observe a net directional current. It is only when the noise intensity is moderate that the coupled motors can move with an optimal collaboration; i.e., an optimized noise intensity G_{max} exists that corresponds to the largest velocity.

6 Concluding remarks

In summary, we studied the mechanism of collaborated directed transport of elastically coupled Brownian motors in a symmetric periodic potential under asynchronous modulations. We applied the effective potential theory and the invariance analysis of space-time transformation of coupled dynamical equations to study the coupling-induced symmetry breaking and its consequent collective directed transport and current-reversal behavior. The effective potential analysis indicates that, for relatively strong coupling strengths, the shifting direction of the effective potential valley eventually determines the availability and direction of ratchet motion, which is further revealed and verified by studying the effective asymmetry coefficient. The dependence of velocity on the coupling free length and pulsation phase shift is also successfully predicted in terms of the space-time transformation invariance analysis, which agrees well with numerical simulations. Moreover, the relations between directed transport on various parameters are investigated systematically, and these results provide a valuable approach of adjusting different parameters in practice for optimizing and manipulating the collective directed transport.

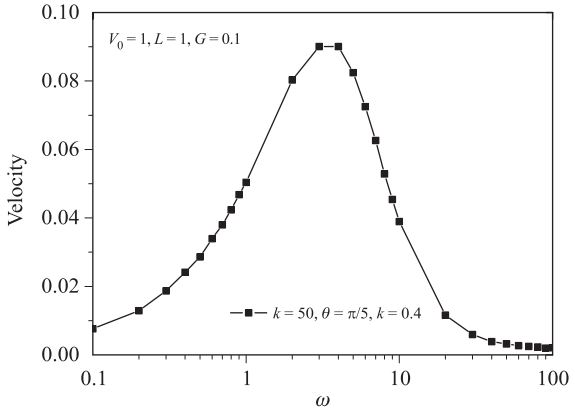

Fig. 7 The average velocity against the pulsating frequency ω.

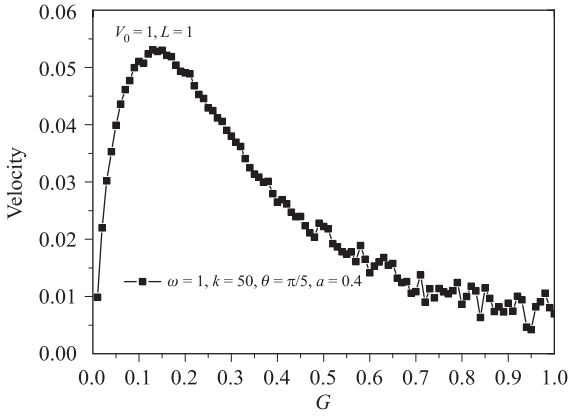

Fig. 8 The influence of the noise intensity on the average velocity.

Acknowledgements This work was partially supported by the National Natural Science Foundation of China (Grant Nos. 11075016 and 11475022) and the Scientific Research Funds of Huaqiao University.

References

1. P. Reimann and M. Evstigneev, Pulsating potential ratchet, *Europhys. Lett.* 78(5), 50004 (2007)
2. F. Marchesoni, Transport properties in disordered ratchet potentials, *Phys. Rev. E* 56(3), 2492 (1997)
3. J. D. Bao and Y. Z. Zhuo, Biasing fluctuation model for directional stepping motion of molecular motor, *Chin. Sci. Bull.* 43(22), 1879 (1998)
4. P. Reimann, Brownian motors: Noisy transport far from equilibrium, *Phys. Rep.* 361(2–4), 57 (2002)
5. H. Y. Wang and J. D. Bao, Kramers-type elastic ratchet model for ATP gating during kinesins mechanochemical cycle, *Physica A* 389(3), 433 (2010)

6. Z. G. Zheng, Directed transport of interacting particle systems: Recent progress, *Commum. Theor. Phys.* 43(1), 107 (2005)
7. B. O. Yan, R. M. Miura, and Y. D. Chen, Direction reversal of fluctuation-induced biased Brownian motion on distorted ratchets, *J. Theor. Biol.* 210(2), 141 (2001)
8. A. Pototsky, N. B. Janson, F. Marchesoni, and S. Savelev, Dipole rectification in an oscillating electric field, *Europhys. Lett.* 88(3), 30003 (2009)
9. Z. G. Zheng, G. Hu, and B. Hu, Collective directional transport in coupled nonlinear oscillators without external bias, *Phys. Rev. Lett.* 86(11), 2273 (2001)
10. S. von Gehlen, M. Evstigneev, and P. Reimann, Ratchet effect of a dimer with broken friction symmetry in a symmetric potential, *Phys. Rev. E* 79(3), 031114 (2009)
11. O. M. Braun, R. Ferrando, and G. E. Tommei, Stimulated diffusion of an adsorbed dimer, *Phys. Rev. E* 68(5), 051101 (2003)
12. S. Gonçalves, C. Fusco, A. R. Bishop, and V. M. Kenkre, Bistability and hysteresis in the sliding friction of a dimer, *Phys. Rev. B* 72(19), 195418 (2005)
13. E. Heinsalu, M. Patriarca, and F. Marchesoni, Dimer diffusion in a washboard potential, *Phys. Rev. E* 77(2), 021129 (2008)
14. A. E. Filippov, J. Klafter, and M. Urbakh, Friction through dynamical formation and rupture of molecular bonds, *Phys. Rev. Lett.* 92(13), 135503 (2004)
15. S. Maier, Y. Sang, T. Filleter, M. Grant, R. Bennewitz, E. Gnecco, and E. Meyer, Fluctuations and jump dynamics in atomic friction experiments, *Phys. Rev. B* 72(24), 245418 (2005)
16. H. Y. Wang and J. D. Bao, Transport coherence in coupled Brownian ratchet, *Physica A* 374(1), 33 (2007)
17. J. L. Mateos, A random walker on a ratchet, *Physica A* 351(1), 79 (2005)
18. S. E. Mangioni and H. S. Wio, A random walker on a ratchet potential: effect of a non Gaussian noise, *Eur. Phys. J. B* 61(1), 67 (2008)
19. E. M. Craig, M. J. Zuckermann, and H. Linke, Mechanical coupling in flashing ratchets, *Phys. Rev. E* 73(5), 051106 (2006)
20. J. Menche and L. Schimansky-Geier, Two particles with bistable coupling on a ratchet, *Phys. Lett. A* 359(2), 90 (2006)
21. M. Evstigneev, S. von Gehlen, and P. Reimann, Interaction-controlled Brownian motion in a tilted periodic potential, *Phys. Rev. E* 79(1), 011116 (2009)
22. C. Lutz, M. Reichert, H. Stark, and C. Bechinger, Surmounting barriers: The benefit of hydrodynamic interactions, *Europhys. Lett.* 74(4), 719 (2006)
23. H. Y. Wang and J. D. Bao, The roles of ratchet in transport of two coupled particles, *Physica A* 337(1–2), 13 (2004)
24. Z. G. Zheng, M. C. Cross, and G. Hu, Collective directed transport of symmetrically coupled lattices in symmetric periodic potentials, *Phys. Rev. Lett.* 89(15), 154102 (2002)
25. Z. G. Zheng and H. B. Chen, Cooperative two-dimensional directed transport, *Europhys. Lett.* 92(3), 30004 (2010)
26. S. von Gehlen, M. Evstigneev, and P. Reimann, Dynamics of a dimer in a symmetric potential: Ratchet effect generated by an internal degree of freedom, *Phys. Rev. E* 77(3), 031136 (2008)
27. A. D. Rogat and K. G. Miler, A role for myosin VI in actin dynamics at sites of membrane remodeling during Drosophila spermatogenesis, *J. Cell Sci.* 115(24), 4855 (2002)
28. H. Park, A. Li, L. Q. Chen, A. Houdusse, P. R. Selvin, and H. L. Sweeney, The unique insert at the end of the myosin VI motor is the sole determinant of directionality, *Proc. Natl. Acad. Sci. USA* 104(3), 778 (2007)
29. E. M. Delacruz, E. M. Ostap, and H. L. Sweeney, Kinetic mechanism and regulation of myosin VI, *J. Biochem.* 276(34), 32373 (2001)
30. S. Nishikawa, K. Homma, Y. Komori, M. Iwaki, T. Wazawa, A. Hikikoshi Iwone, J. Saito, R. Ikebe, E. Katayama, T. Yanagida, and M. Ikebe, Class VI myosin moves processively along Actin filaments backward with large steps, *Biochem. Biophys. Res. Commun.* 290(1), 311 (2002)
31. J. C. Chen and G. Z. Su, Thermodynamics and Statistical Physics (Vol.1), Beijing: Science Press, 2010, pp 268–282
32. J. D. Bao, Stochastic Simulation Method of Classical and Quantum Dissipative Systems, Beijing: Science Press, 2009, pp 102–135
33. Z. G. Zheng, Collective Behaviors and Spatiotemporal Dynamics in Coupled Nonlinear System, Beijing: Higher Education Press, 2004, pp 278–347
34. H. B. Chen, Q. W. Wang, and Z. G. Zheng, Deterministic directed transport of inertial particles in a flashing ratchet potential, *Phys. Rev. E* 71(3), 031102 (2005)